



Research Article

GPA33 is expressed on multiple human blood cell types and distinguishes CD4⁺ central memory T cells with and without effector function

Rianne Opstelten¹ , Jessica S Suwandi², Manon C. Slot¹,
Florenca Morgana¹, Andrew M Scott³, Sandra Laban², Tatjana Nikolic²,
Annelies W Turksma⁴, Anna Kroeze^{1,4}, Carlijn Voermans¹,
Jaap-Jan Zwaginga^{2,5}, Bart O Roep^{2,6} and Derk Amsen^{1,7} 

¹ Department of Hematopoiesis and Department of Immunopathology, Sanquin Research and Landsteiner Laboratory, Amsterdam UMC, University of Amsterdam, Amsterdam, the Netherlands

² Immunomodulation and Regenerative Cell Therapy, Department of Internal Medicine, Leiden University Medical Center, Leiden, Netherlands

³ Tumour Targeting Laboratory, Olivia Newton-John Cancer Research Institute, and School of Cancer Medicine, La Trobe University, Melbourne, Australia

⁴ Department of Immunopathology, Sanquin Research and Landsteiner Laboratory, Amsterdam UMC, University of Amsterdam, Amsterdam, the Netherlands

⁵ Sanquin Research, Center for Clinical Transfusion Research and Jon J van Rood Center for Clinical Transfusion Science, Leiden University Medical Center, Leiden, Netherlands

⁶ Department of Diabetes Immunology, Diabetes & Metabolism Research Institute at the Beckman Research Institute, City of Hope, Duarte, CA, USA

⁷ Department of Experimental Immunology, Amsterdam UMC, University of Amsterdam, Amsterdam, the Netherlands

The Ig superfamily protein glycoprotein A33 (GPA33) has been implicated in immune dysregulation, but little is known about its expression in the immune compartment. Here, we comprehensively determined GPA33 expression patterns on human blood leukocyte subsets, using mass and flow cytometry. We found that GPA33 was expressed on fractions of B, dendritic, natural killer and innate lymphoid cells. Most prominent expression was found in the CD4⁺ T cell compartment. Naïve and CXCR5⁺ regulatory T cells were GPA33^{high}, and naïve conventional CD4⁺ T cells expressed intermediate GPA33 levels. The expression pattern of GPA33 identified functional heterogeneity within the CD4⁺ central memory T cell (Tcm) population. GPA33⁺ CD4⁺ Tcm cells were fully undifferentiated, *bona fide* Tcm cells that lack immediate effector function, whereas GPA33⁻ Tcm cells exhibited rapid effector functions and may represent an early stage of differentiation into effector/effector memory T cells before loss of CD62L. Expression of GPA33 in conventional CD4⁺ T cells suggests a role in localization and/or preservation of an undifferentiated state. These results form a basis to study the function of GPA33 and show it to be a useful marker to discriminate between different cellular subsets, especially in the CD4⁺ T cell lineage.

Correspondence: Derk Amsen
e-mail: d.amsen@amsterdamumc.nl; d.amsen@sanquin.nl

Keywords: antibody therapy · CD4⁺ T cell differentiation · CyTOF · flow cytometry · human glycoprotein A33



Additional supporting information may be found online in the Supporting Information section at the end of the article.

Introduction

Transmembrane proteins of the Ig superfamily are characterized by the presence of one or more extracellular Ig domains and have a diversity of functions in cellular communication and adhesion. In addition to the antigen receptors on B cells and T cells, various Ig domain proteins control cellular adhesion, activation, and differentiation [1]. The glycoprotein A33 (GPA33) was first described as an Ig super family member of the cortical thymocyte marker for *Xenopus* (CTX) group of type I transmembrane proteins [2]. GPA33 has high homology with CD2 and contains a V-type Ig-like domain at the N terminus [3]. It is also related to proteins that have inhibitory roles in T cell activation, such as CD276 (B7-H3) [4] and VSIG4 [5] and several cell adhesion molecules, such as CEACAM, ICAM, and NCAM (3D-Protein BLAST, NCBI). Although its molecular function is not known, GPA33 has been associated with immune dysregulation. Genetic linkage has been found between polymorphisms in the gene encoding GPA33 and the autoimmune disorder eosinophilic granulomatosis with polyangiitis [6]. Furthermore, the *GPA33* gene is located in a susceptibility locus for Sjögren's Syndrome [7]. A mouse KO model of GPA33 exhibited hypersensitivity to food allergens [8] and excessive inflammatory responses to artificially induced colitis [9]. Establishing the complete expression pattern of this molecule will be a useful stepping stone for further studies into the function of this molecule, both in normal physiology and in disease. Furthermore, information on the expression pattern of GPA33 may help assess the risks of targeting this molecule for therapeutic purposes, for instance using bispecific antibodies [10] directed against GPA33 and CD3, which aim to target activated T cells to colorectal carcinomas [11,12].

For these reasons, we here performed a comprehensive analysis of the GPA33 expression pattern among white blood cells in human blood. We show that GPA33 is prominently expressed on several conventional and regulatory CD4⁺ T cell types, and that minor subsets of CD8⁺ T cells, B cells, dendritic cells (DCs), innate lymphoid cells (ILCs), and natural killer (NK) T cells are also GPA33⁺. Most strikingly, we report that the GPA33 expression pattern reveals functional heterogeneity among CD4⁺ central memory T cells (Tcm). This population of memory T cells with high proliferative capacity is thought to preserve the ability to differentiate into various effector cell lineages and to serve as a reservoir for the generation of new effector T cells during recall infections [13]. We show that GPA33 is a marker that can be used to separate bona fide Tcm cells without effector function from Tcm cells that appear already committed to developing effector function and may recently have been activated. These results set the stage for further studies into the function of this protein in

these cell types and are important for therapies that intend to target this molecule for clinical purposes. Finally, they reveal GPA33 as a useful marker to identify Tcm cells that have not committed to effector differentiation.

Results

CyTOF reveals GPA33 expression in several immune cell types in human blood

In order to comprehensively characterize expression of GPA33 on leukocyte subsets, we measured surface expression of 39 markers on total PBMCs from a healthy donor using CyTOF technology (see Table S3). An initial Hierarchical Stochastic Neighbor Embedding (HSNE) analysis of the CyTOF data identified five main lineages of cells, namely CD4⁺ T cells (CD3⁺ CD4⁺), CD8⁺ T cells (CD3⁺ CD8⁺), Monocytes (CD3⁻ HLA-DR⁺ CD4^{dim}), B cells (CD3⁻ HLA-DR⁺ CD4⁻), and NK cells (CD3⁻ HLA-DR⁻ CD57⁺) (Fig. 1A). TCRγδ T cells were also visible as a (small) separate cluster within the CD8⁺ T cell cluster. Plotting the intensity of GPA33 staining on these populations showed that this receptor (Fig. 1A; lower right panel) was most prominently expressed among CD4⁺ T cells. However, zooming in on each lineage (Fig. 1B), demonstrated some GPA33 expression in subsets of CD8⁺ T cells, Monocytes, B cells and NK cells, albeit to a much lesser extent, both in intensity and frequency.

GPA33 is expressed on B cell subsets

To further characterize the expression pattern of GPA33 on leukocyte subsets, we made use of specially designed panels of antibodies that allow analysis by regular flow cytometry (A. Kroeze, A. W. Turksma, N. Weterings, D. Stalder, C. Homburg, A. ten Brinke, C.E. van der Schoot, S.S. Zeerleder, C. Voermans, Cellular subsets in acute Graft-versus-Host disease, manuscript in preparation). We used CD19, CD27, IgD and CD38 to identify naïve, non-switched B cells, switched B cells and plasma blasts (see Figure S3 and Table S1 for details on gating strategy) [14]. Figure 2A shows that fractions of all B cell subsets expressed GPA33, with the smallest fractions found among switched and non-switched memory B cells (for validation of anti-GPA33 antibody staining specificity in this population and other populations examined in this manuscript, see Figure S1A and B). The intensity of GPA33 staining found in naïve B cells was somewhat lower than that among switched memory B cells and plasma blasts. High expression of

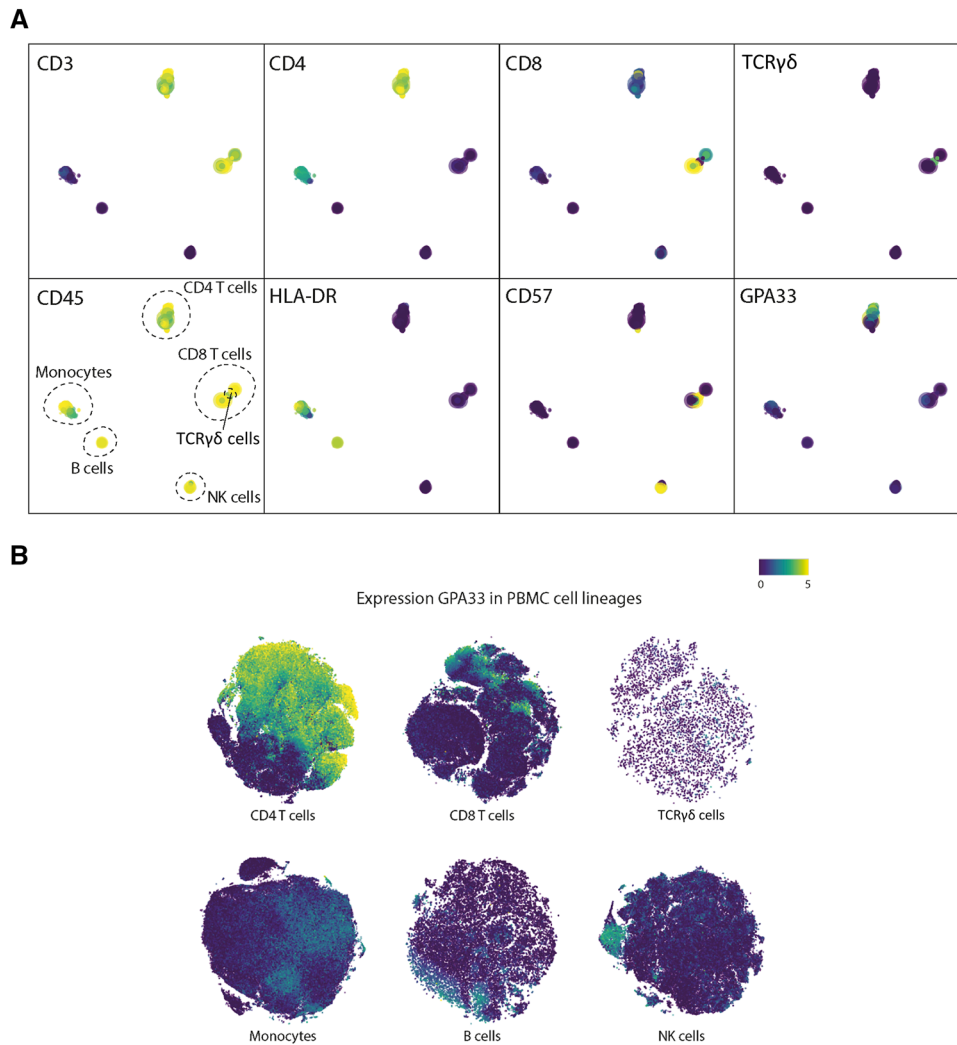


Figure 1. Investigating GPA33 expression on human PBMCs with CyTOF. **(A)** Hierarchical Stochastic Neighbor Embedding (HSNE) analysis of the CyTOF data from total PBMCs. Shown are the signal intensities for the markers listed in the top left corner of each panel (scale below figure). This clustering distinguishes 5 major lineages of cells: CD4⁺ T cells (defined as CD3⁺ CD4⁺), CD8⁺ T cells (defined as CD3⁺ CD8⁺), Monocytes (defined as CD3⁻ HLA-DR⁺ CD4⁺), B cells (defined as CD3⁻ HLA-DR⁺ CD4⁻) and NK cells (defined as CD3⁻ CD57⁺). Cell types are labeled in the CD45 intensity plot. The TCR $\gamma\delta$ T cell subset is found within the larger CD8⁺ T cell cluster. **(B)** GPA33 expression projected on HSNE plots at the single-cell data level for each lineage. Data show one experiment from one technical replicate with one donor. For antibodies used, see Table S3.

GPA33 was only observed among CD27^{high} memory B cells. CD27⁻ B cells exhibited lower intensity staining (Fig. 2B), while hardly any GPA33 expression was seen among cells expressing intermediate levels of CD27. Strikingly, the CD19⁺CD27^{high}GPA33^{high} cells largely lack expression of IgM, IgD, IgA, and IgG when compared to the total memory population. These GPA33⁺ memory B cells may therefore produce IgE, but this possibility remains to be tested.

GPA33 is expressed on minor fractions of mDC2, NKT, ILC1, CD4⁺CD8⁺, and CD4⁻CD8⁻ T cells

Dendritic cells (DCs) were gated from the CD56⁻HLA-DR⁺ population and further subdivided into (CD123⁺) plasma-

cytoid(p)DCs, (Slan-MD8⁺) Slan DCs, and (CD1c⁺) myeloid (m)DC1 and (CD141⁺) mDC2 (Figure S3 and Table S1). Only the mDC2 subset contained a sizeable population expressing GPA33, albeit not with very high intensity (Figure 3A and S1). Monocytes were identified as HLA-DR⁺CD11c⁺M-DC8⁻, and then further divided based on expression of CD14 and CD16 (Figure S3 and Table S1). We found the classical (CD14⁺CD16⁻), intermediate (CD14⁺CD16⁺), as well as the non-classical (CD14⁻CD16⁺) monocytes to be largely negative for GPA33 (Fig. 3B).

The CD3⁻CD14⁻ NK cell population was divided into three subsets based on the expression of CD56 and CD16 (Figure S3 and Table S1). Low intensity GPA33 staining was found among the more mature CD56^{dim} NK cell subset (CD56^{+/-}), but was absent from the CD56^{bright} (CD56^{+/+}) NK cells (Figure 4A and

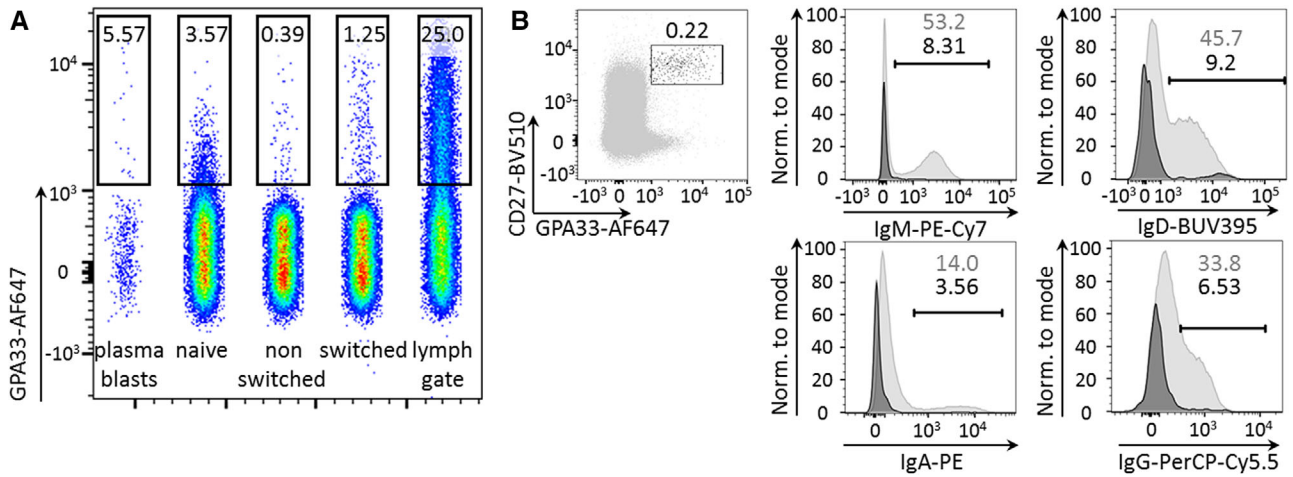


Figure 2. GPA33⁺ subsets in major human B cell lineages. (A) CD19⁺ B cells, delineated from PBMCs, were divided into naive, non-switched memory and switched memory B cells based on the expression of CD27 and IgD (see Figure S3A for gating strategy). Plasma blasts were identified as IgD⁻, CD27^{high}, and CD38^{high}. A concatenated dot plot from a representative donor with GPA33 on the y-axis of all B cell populations is shown. GPA33 expression of total lymphoid cells is shown as positive control (lymph gate). Numbers above the gates indicate the percentage of GPA33⁺ cells in that particular subset. (B) Dot plot of CD27 against GPA33 of the total CD19⁺ population (grey) reveals a CD27⁺ population that expresses GPA33 (black). Overlaid histograms of CD27⁺ B cells (grey) and CD27⁺GPA33⁺ B cells (black) for different antibody isotypes are shown on the right. The upper numbers in graphs (dark grey) refer to the percentage of cells in the total CD27⁺ memory population that are positive for each Ig. The lower numbers (black) give the same percentage for the CD27⁺GPA33⁺ population. A representative donor of *n* = 4 from one technical replicate of four independent experiments is shown. All experiments were measured by flow cytometry and for antibodies used, see Table S2.

Figure S1). A third, less well known and mostly anergic subset of NK cells [15], marked by a CD56⁻CD16⁺ NK phenotype, also contained a small fraction of cells weakly expressing GPA33, similar to the CD56^{bright} NK cells. Finally, about 15% of the CD56⁺CD3⁺ NKT cells were positive for GPA33. Innate lymphoid cells (ILC) were gated as CD45⁺Lineage⁻CD3⁻CD127⁺ and then further

subdivided on the basis of CD294, CD161, CD117 and Nkp44 [16,17] (Figure S3 and Table S1). As shown in Figure 4B, the only subpopulation among ILCs that convincingly contained GPA33 positive cells was the ILC1 population (~20%). NKp44⁺ ILC3 cells were only found in one donor, and are therefore described in Table S4.

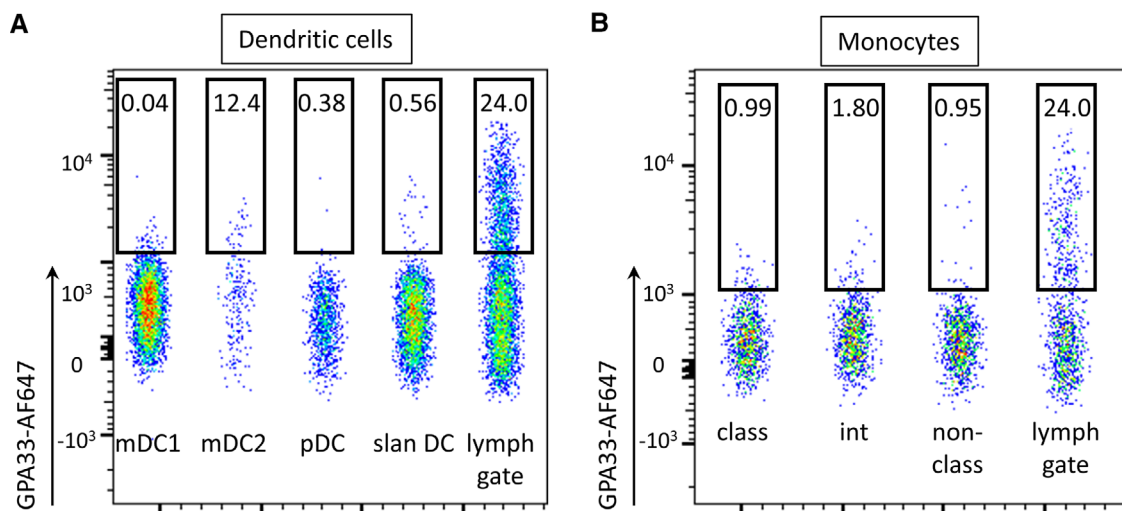


Figure 3. Little GPA33 is expressed on human DC's and monocytes. (A) Concatenated dot plots from a representative donor of GPA33 expression in DC subsets. DC's were gated from total PBMCs as HLA-DR⁺CD56⁻, mDC1's as CD11c⁺CD141⁻ and mDC2's as CD11c⁺CD141⁺. pDC's were gated as CD123⁺ and slanDC's were Slan MD-8⁺. GPA33 expression of total lymphoid cells is shown as positive control (lymph gate – also in (B)). Numbers above the gates indicate the percentage of GPA33⁺ cells in that particular subset. (B) Concatenated dot plots from a representative donor of GPA33 expression in monocytes. Monocytes were defined from total PBMCs as CD11c⁺HLA-DR⁺Slan MD-8⁻ and were further subdivided based on the expression of CD14 and CD16 (see Figure S3A for gating strategy). Numbers above the gates indicate the percentage of GPA33⁺ cells in that particular subset. A representative donor of *n* = 4 from one technical replicate of 4 independent experiments is shown. All experiments were measured by flow cytometry and for antibodies used, see Table S2.

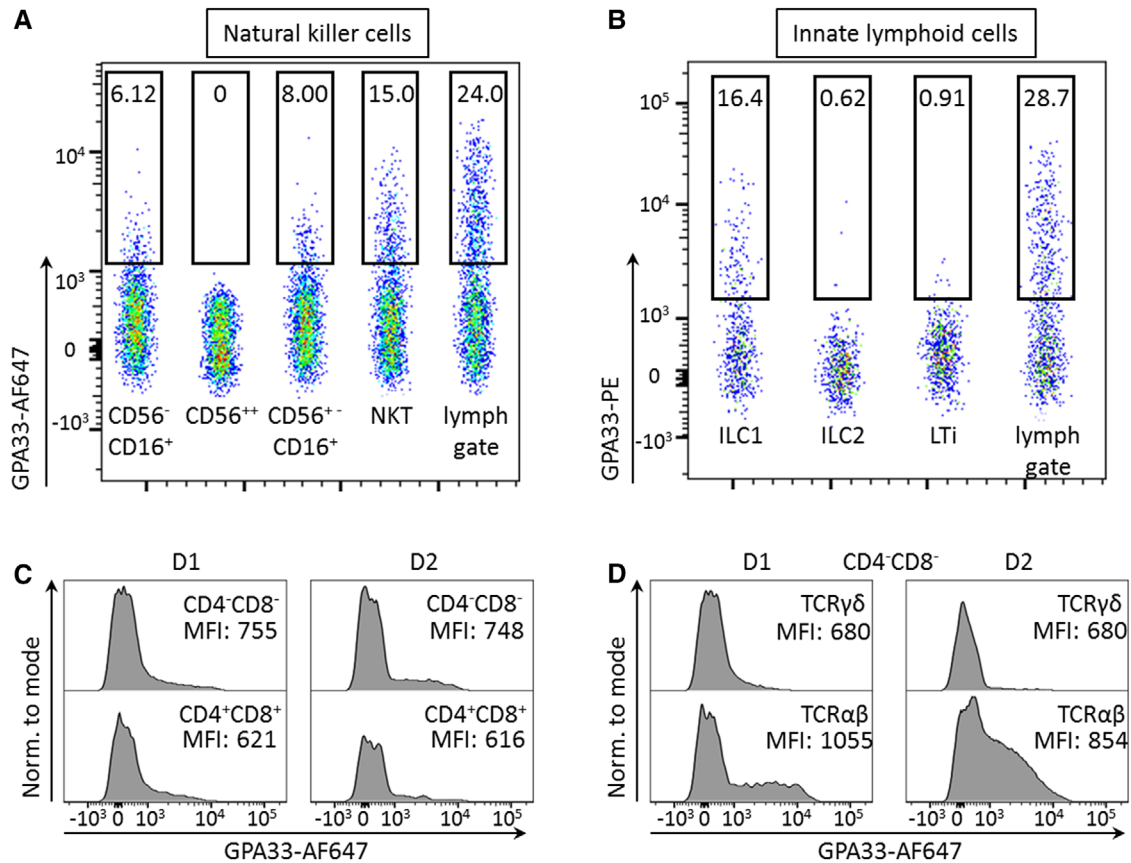


Figure 4. GPA33 expression is most pronounced on human NKT cells and ILC1's and is restricted to T cells with an $\alpha\beta$ TCR. (A) Concatenated dot plots from a representative donor of GPA33 expression in NK(T) subsets. NK cells were delineated from total PBMCs as CD3⁺CD14⁻, except for NKT cells, which are CD3⁺CD56⁺. Subsets were gated based on expression of CD56 and CD16 as indicated in the figure. GPA33 expression of total lymphoid cells is shown as positive control (lymph gate-also in B). Numbers above the gates indicate the percentage of GPA33⁺ cells in that particular subset. (B) Concatenated dot plots from a representative donor of GPA33 expression in ILC subsets. ILCs were gated from total PBMCs as CD45⁺Lin⁻CD3⁻CD127⁺CD161⁺ and then gated as CD294⁺ ILC2's, CD117⁺ LTi's and CD117⁻ ILC1's. Numbers above the gates indicate the percentage of GPA33⁺ cells in that particular subset. NKp44⁺ ILC3 cells were only found in one donor, and are therefore described in the supplementary data (Table S4c). A representative donor of $n = 4$ is shown. (C) Histograms of GPA33 expression on CD4⁻CD8⁻ and CD4⁺CD8⁺ of two representative donors (D1 & D2). (D) Histograms of two representative donors (D1 and D2) showing GPA33 expression on TCR $\gamma\delta$ cells and TCR $\alpha\beta$ cells within the CD4⁻CD8⁻ subset. One or two representative donors of $n = 4$ from one technical replicate of four independent experiments are shown. All experiments were measured by flow cytometry and for antibodies used, see Table S2.

Fractions of GPA33⁺ cells among the populations examined thus far were often small. To corroborate the presence of GPA33 in these populations, we examined expression of GPA33 mRNA in the Human Cell Atlas database (<https://www.humancellatlas.org/>; Figure S2). In all cell populations where GPA33 expression was detected by FACS, expression was indeed documented by measurement of mRNA, reinforcing the validity of our results.

Besides the conventional CD4⁺ and CD8⁺ T cells, there are two other, less well understood populations of CD3⁺ cells. CD4⁺CD8⁺ T cells have been found in many different species, and (in humans) in various peripheral tissues [18]. The function of these cells remains elusive, and seemingly contradictory functions have been attributed to these cells, ranging from suppressive capacity to strong effector function [18]. Figure 4C shows that a small fraction of these cells was weakly positive for GPA33. A low number of GPA33⁺ cells is also found among CD4⁻CD8⁻ T cells, but was

restricted to cells expressing an $\alpha\beta$ TCR and absent from TCR $\gamma\delta$ T cell (Fig. 4D). Similar expression patterns were observed with the CyTOF analysis (Figure S5).

GPA33 is associated with differentiation status in CD4⁺ T cells

As already indicated by the CyTOF analysis on leukocyte subsets (Fig. 1), expression of GPA33 was most pronounced on T cells, especially on those expressing CD4, compared to other peripheral leukocytes. GPA33 expression among CD8⁺ T cells was limited (Figure S5). A HSNE map of all subpopulations within the CD4⁺ T cells (Fig. 5) demonstrated that clusters 4, 12 - 18 and 20 - 25 express GPA33 (Fig. 5; a heatmap of these clusters is shown in Figure S4). Among these, the highest expression of GPA33 was found in cluster 22, which together with

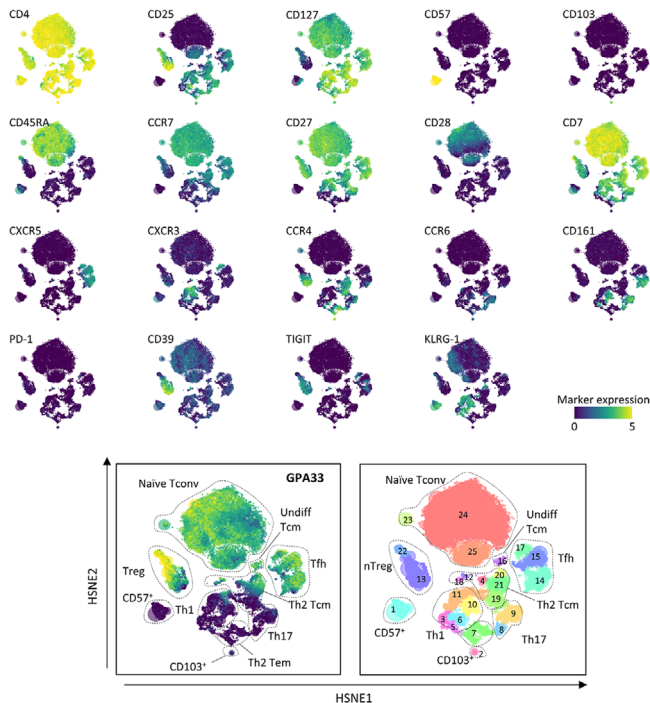


Figure 5. HSNE analysis of total PBMCs reveals differential GPA33 expression on human CD4⁺ T cell populations. Shown are the relative signal intensities for the markers listed in the top left corner of each panel (scale below figure). Cell types are labelled in the GPA33 intensity plot at the bottom left. All cluster numbers are shown in the plot on the bottom right and also respond to the heatmap shown in Figure S4. Data show one experiment with one technical replicate of one donor. For antibodies used, see Table S3.

cluster 13 shows high CD25 expression and low/intermediate levels of CD127 (presumably containing Treg cells). Cluster 22 contains CD127^{low}CD25⁺CD45RA⁺ (naïve) Treg cells, and their high GPA33 expression found by CyTOF is in line with our previous results that reported high GPA33 expression with flow cytometry [19]. Cells in cluster 13 showed intermediate to high expression of GPA33. This cluster consists of CD127^{low}CD25⁺CD45RA⁻ (effector Treg cells) and cells expressing intermediate CD25 and low CD127 (termed Fraction III [20]). These results were confirmed by flow cytometry (Fig. 6A).

Three CD4⁺ T cell clusters (14, 15, and 17) exhibited co-expression of GPA33 with CXCR5. This chemokine receptor is necessary for the function of T follicular helper cells (Tfh), which regulate Ig isotype class switching and somatic hypermutation by activated B cells in germinal centers [21]. Indeed, flow cytometry analysis confirmed that a large proportion of CD4⁺CXCR5⁺PD1⁺ T cells (but not CD8⁺CXCR5⁺PD1⁺ T cells [22]) in blood expresses GPA33 (Fig. 6B). Interestingly, GPA33 was also found on CD4⁺CD25⁺CXCR5⁺PD1⁺ T cells (Fig. 6B), which resemble T follicular regulatory cells (Tfr), a subset of specialized Treg cells that help shape the GC response through interactions with Tfh [21].

In clusters 23–25 (Fig. 5), GPA33 was strongly co-expressed with CD45RA, CD27, and CCR7 and exhibited an inverse expression pattern with activation markers, such as CD39 and TIGIT.

This suggests that GPA33 is expressed by naïve T cells, but not by populations with an effector phenotype. The GPA33⁺ clusters 16, 20, and 21 were also CCR7⁺ and CD27⁺, but CD45RA⁻, indicating that the CD4⁺ central memory (Tcm) population expresses GPA33. We verified these results by conventional flow cytometry. Figure 7A shows GPA33 FACS plots for CD4⁺ and CD8⁺ T cell subsets (for gating, see Figure S3 and Table S1) ranging from least differentiated at the top (true CD27⁺CD28⁺ naïve) to most differentiated (effector) at the bottom. CD8⁺ T cells show low expression of GPA33 when measured by flow cytometry, comparable to the signal detected with CyTOF (Fig. 7A and Fig. S5), and expression of GPA33 did not seem to be restricted to specific subsets (Fig. 7A). In contrast, marked expression of GPA33 was detected in specific subsets of CD4⁺ T cells. As anticipated from the CyTOF data, the entire naïve CD4⁺ population expressed GPA33, and this marker was also expressed in the Tcm CD4⁺ T cell population (quantified in Fig. 7B). In agreement with the apparent inverse association of GPA33 with effector differentiation in CD4⁺ T cells, expression of GPA33 correlated inversely with the capacity to produce effector cytokines, such as IFN γ and IL17, after stimulation with PMA+Ionomycin (Fig. 7C). Such an inverse relationship is not observed, however, with production of IL-2, which can also abundantly be produced by naïve CD4⁺ T cells [23].

Tcm cells are a population of memory T cells with high proliferative capacity and limited ability to exhibit immediate effector function (production of cytokines such as IFN γ and IL-17), in contrast to effector memory T (Tem) cells, which exhibit the opposite characteristics [13]. As such, Tcm cells have been compared to stem cells [24], by virtue of their capacity to self-renew and to generate new populations of effector T cells and Tem cells during recall infections. Our results revealed that this population is heterogeneous with regard to expression of GPA33 (Fig. 7A). Given the correlation between GPA33 expression and lack of effector function in the CD4⁺ T cell population (naïve Tregs, naïve conventional T cells, Tcm cells), we hypothesized that GPA33 might mark the *bona fide* resting Tcm cells, whereas GPA33⁻ Tcm cells might be underway to differentiate into Tem cells. In agreement with this idea, GPA33⁻ cells in the CD4⁺ Tcm population exhibited lower expression of the chemokine receptor CCR7 than GPA33⁺ CD4⁺ Tcm, and contained a greater proportion of cells expressing the T helper 1 associated chemokine receptor CXCR3 [25] (Fig. 8A,B). When mimicking TCR stimulation in CD4⁺ Tconv cells via CD3 and CD28, a downregulation of GPA33 was observed (Fig. 8C). Therefore, Tcm cells were FACSsorted into GPA33⁺ and GPA33⁻ cells before assessing the effects of TCR stimulation on markers associated with effector differentiation, like the transcription factor T-bet [26], and the T helper 2 associated chemokine receptor CCR4 (Fig. 8D). Both were induced much more readily in GPA33⁻ than in GPA33⁺ CD4⁺ Tcm (Fig. 8D). Finally, GPA33⁻ CD4⁺ Tcm produced the effector cytokines IL-17 and IFN γ during short term stimulation with PMA and ionomycin, whereas GPA33⁺ Tcm cells largely lacked this ability (Fig. 8E; please note that GPA33 expression was not affected by these short term activation conditions, allowing analysis of Tcm cells without prior isolation of GPA33⁺ and GPA33⁻ cells). In contrast, no significant difference

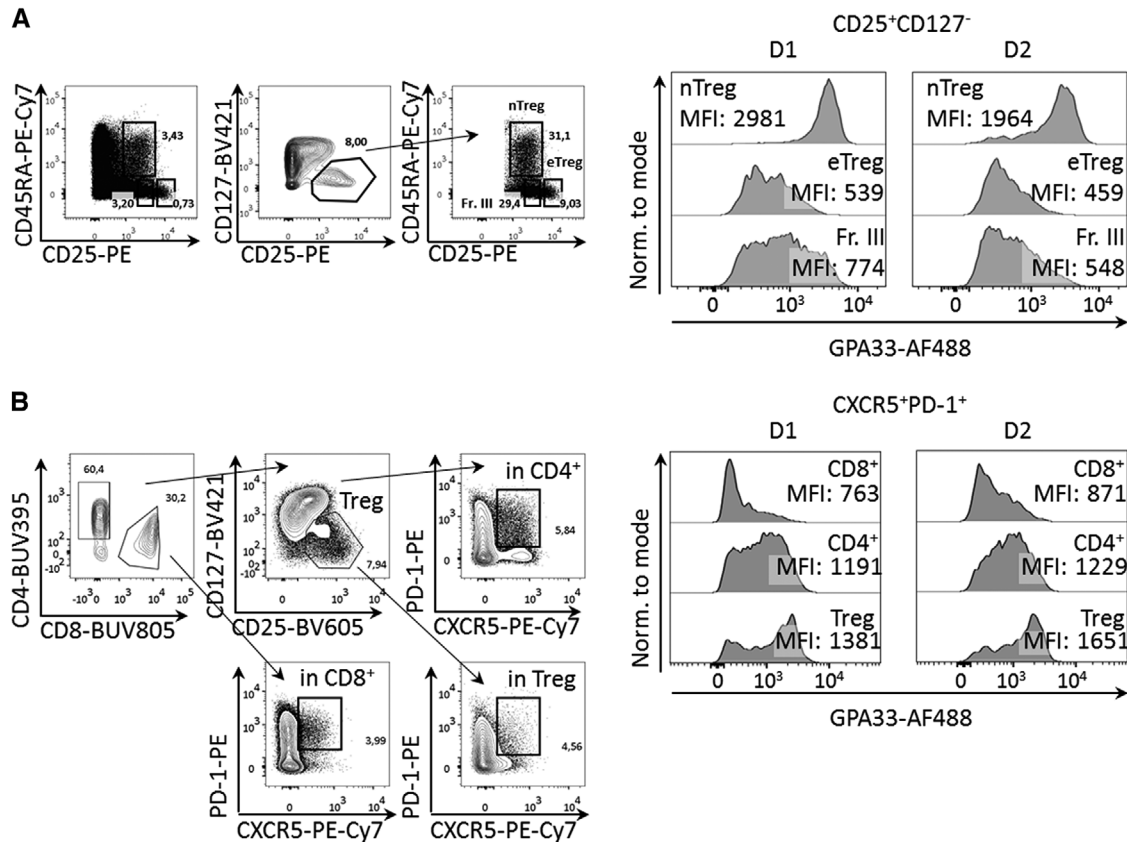


Figure 6. GPA33 is expressed on human regulatory T cells and on CD4⁺ Tfh and Tfr, but not on CD8⁺ Tfh. **A)** Gating strategy for CD4⁺CD25⁺CD127⁻Treg cells from total PBMCs, starting from the lymphocyte single cell live CD4⁺ gate (left). Histograms of GPA33 expression in CD25⁺CD127⁻CD45RA⁺ nTreg cells, CD25^{hi}CD127⁻CD45RA⁻ eTreg and CD25⁺CD127⁻CD45RA⁻ Fr. III cells for two representative donors (D1 & D2; right). **(B)** Gating strategy for defining Tfh and Tfr, starting from the lymphocyte single cell live CD14⁻CD45⁺CD3⁺ T cell population (left). Histograms of GPA33 expression in CD4⁺ and CD8⁺ Tfh and CD4⁺ Tfr, defined as CXCR5⁺PD-1⁺ cells within the appropriate gate, for two representative donors (D1 & D2; right). Two representative donors of $n = 4$ from one technical replicate of four independent experiments are shown. All experiments were measured by flow cytometry and for antibodies used, see Table S2.

was found between these CD4⁺ Tcm subsets in the ability to produce IL-2 (Fig. 8E), which is produced by Tcm and Tem cells alike [27].

GPA33⁻ CD4⁺ T cells in the Tcm gate were not fully differentiated Tem: while their CCR7 expression intensity was clearly lower than that on the GPA33⁺ cells in the Tcm gate, it was still markedly higher than on the Tem population (Fig. 8B). Furthermore, expression of the lymphoid tissue homing receptor CD62L was clearly more prominent on GPA33⁻ Tcm cells than on genuine Tem cells and actually resembled that on GPA33⁺ Tcm cells (Fig. 8B). Finally, GPA33⁺ and GPA33⁻ Tcm cells possessed similar proliferative capacity after stimulation via the TCR and CD28 (results not shown). These results are consistent with the hypothesis that loss of GPA33, an event that can be triggered by TCR stimulation (Fig. 8C), marks Tcm cells that have been stimulated to develop into Tem cells.

Thus, within the CD4⁺ CD45RA⁻ CCR7⁺ population, those cells that express GPA33 correspond best to the classical definition of Tcm cells, while loss of this marker may be an early sign of differentiation into cells with effector functions.

Discussion

In this study, we determined the expression of GPA33 in human mononuclear blood leukocytes using CyTOF and flow cytometry. Various populations of cells (several types of B cells, DC, monocytes and NK cells) exhibited either weak expression of this molecule or contained only small proportions of GPA33⁺ cells. Staining on these populations was higher than obtained with the appropriate isotype controls, but more detailed studies will be required to document whether this staining represents true expression by these cells. The fact that GPA33 mRNA could be detected in these populations is at least consistent with endogenous expression of this marker. However, other possibilities include protein acquisition through trogocytosis or from exosomes [28,29]. Somewhat larger fractions of GPA33⁺ cells (in the range of 10 to 20%) were found among mDC2, NKT cells, and ILC1. Most prominent expression was found, however, on T cells, and CD4⁺ T cells in particular. Although some CD4⁺CD8⁻ and CD8⁺ $\alpha\beta$ T cells expressed GPA33, the largest GPA33⁺ fractions were found among naïve and follicular Tregs as well as among

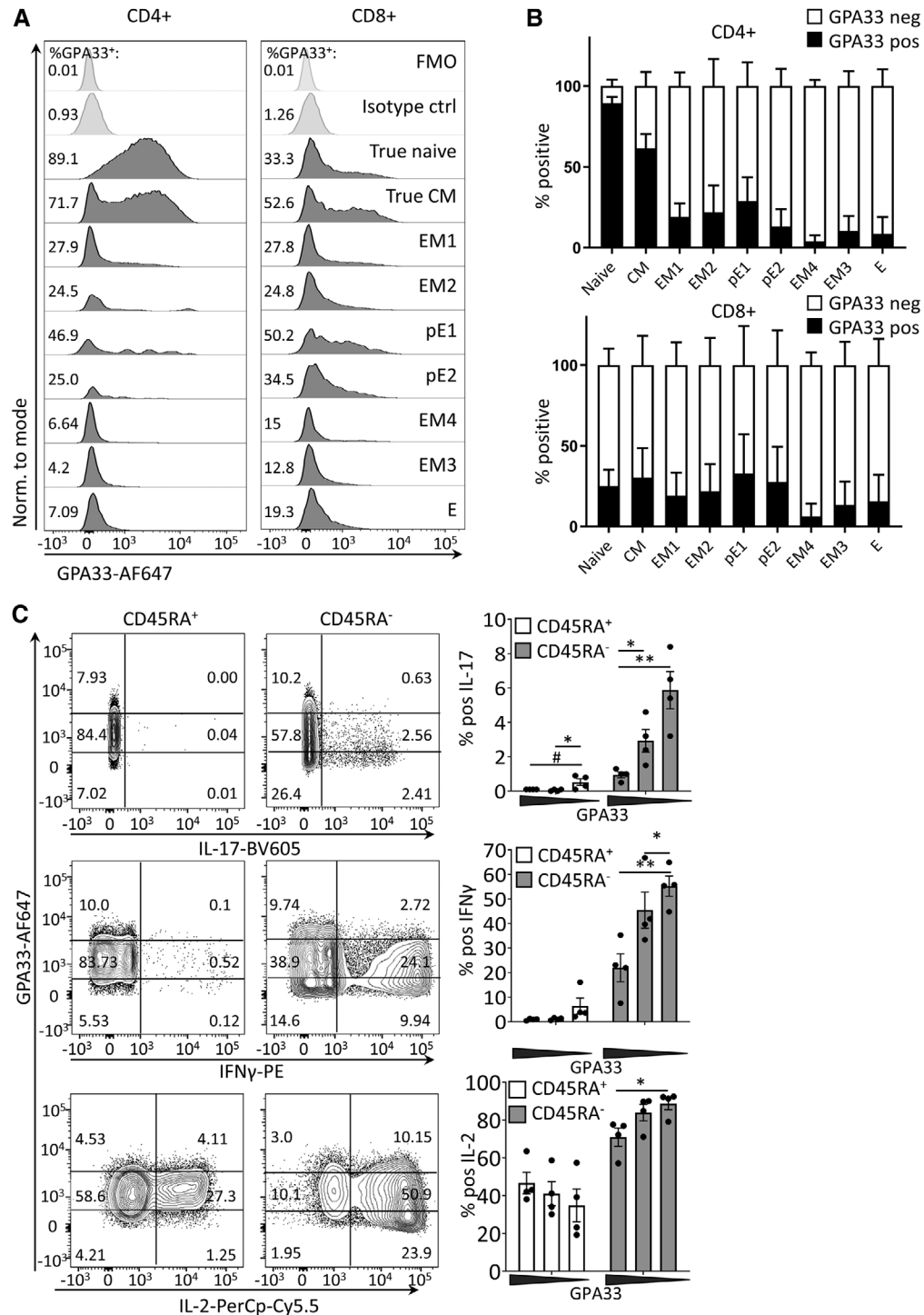


Figure 7. GPA33 is associated with an undifferentiated phenotype in human CD4⁺ cells. (A) Histograms from a representative donor of one technical replicate from one experiment ($n = 5$ donors) showing expression of GPA33 in live, single CD3⁺CD4⁺ (left) and CD3⁺CD8⁺ (right) T cell subsets (defined in Figure S3E). The experiment was performed using flow cytometry and for antibodies used, see Table S2. (B) Quantification of GPA33⁺ (black) and GPA33⁻ (white) cells in the CD4⁺ (top) and CD8⁺ (bottom) T cells subsets from (A) in all five donors. (C) Intracellular staining for IL-17, IFN- γ , and IL-2 plotted against GPA33 after 4h PMA+IO stimulation of CD4⁺ cells for the FACSsorted CD45RA⁺CD25^{lo} and the CD45RA⁻CD25^{lo} fractions. The graphs on the right of the flow cytometry plots depict the average production of each effector cytokine per GPA33 intensity (high to low, left to right on graphs) for four donors for one technical replicate from one experiment. Error bars represent mean \pm SD. Statistical comparisons were performed by one-way ANOVA, followed by Tukey's HSD. # $p < 0.1$, * $p < 0.05$, ** $p < 0.01$. (for IL-17 in CD45RA⁺CD25^{lo}: GPA33^{hi} vs GPA33^{low} $p = 0.0609$; GPA33^{int} vs GPA33^{low} $p = 0.0373$; for IL-17 in CD45RA⁻CD25^{lo}: GPA33^{hi} vs GPA33^{low} $p = 0.0028$; GPA33^{int} vs GPA33^{low} $p = 0.0477$; for IFN- γ in CD45RA⁻CD25^{lo}: GPA33^{hi} vs GPA33^{int} $p = 0.0470$; GPA33^{hi} vs GPA33^{low} $p = 0.0077$; for IL-2 in CD45RA⁻CD25^{lo}: GPA33^{hi} vs GPA33^{low} $p = 0.0361$).

conventional CD4⁺ naïve, central memory, and follicular helper T cells.

This expression pattern yields several leads regarding the putative function of this receptor. First, the prominent expression in subsets of Treg cells suggests that this molecule may have a role in proper immune regulation, which could explain the association between genetic polymorphisms and various autoimmune conditions [6,7]. The ineffective induction of immunological tolerance in GPA33 deficient mice is consistent with this idea [6–9]. It should be noted, however, that we currently do not know whether the expression pattern of GPA33 is similar between mice and humans.

Suggestive is especially the subdivision of GPA33⁺ naïve-like central memory CD4⁺ T cells, and GPA33⁻ Tcm that exhibit early signs of differentiating into effector memory T cells. Both naïve CD4⁺ T cells and GPA33⁺ Tcm lack immediate ability to produce effector cytokines [30,31]. Shared expression of GPA33 on these cells might point to a function for GPA33 in the maintenance of quiescence and/or prevention of differentiation, as has been reported for the Ig superfamily protein VISTA [32]. Moreover, naïve and central memory T cells share a preference for homing to T cell areas in lymphoid organs, due to expression of CD62L and CCR7 [30,33] and it is conceivable that GPA33 contributes to the homing of these cells to specific niches. Such a role for GPA33 would fit also with its expression on naïve Treg cells, which prevent spurious activation of autoreactive naïve Tconv [34] and should therefore presumably reside in the vicinity of the latter cells. Likewise, the shared GPA33 expression on both subsets of CXCR5⁺PD1⁺ CD4⁺ T cells, those resembling Tfh cells and those resembling Tfr cells, might help position these cells in the same areas in follicular lymphoid tissue. GPA33 expression is also found on all B cell subsets, regardless of differentiation status. Since B cells also home to lymphoid follicles, GPA33 expression may give B cells the same homing potential as it does to T cells.

The expression of GPA33 on naïve and CD4⁺ Tcm cells is lost upon stimulation via TCR and CD28. This suggests that the GPA33⁻ Tcm population may derive from GPA33⁺ Tcm precursors that have recently been activated. If this interpretation is correct, it is interesting that loss of GPA33 occurs before loss of CD62L. Expression of this receptor would in principle allow these cells (which, as our analysis shows, are present in peripheral blood) to re-enter lymphoid tissues via high endothelial venules [35]. The loss of CCR7 (and perhaps GPA33) would, however, target these cells to different regions in such tissues than genuine GPA33⁺CCR7^{high} Tcm cells, such that GPA33⁻ Tcm cells might be destined to contribute to the lymphoid Tcm population. Regardless of the function of GPA33, our data show that this surface molecule can be used as a marker to distinguish Tcm cells with different properties and are likely at different stages of effector differentiation.

In conclusion, GPA33 is expressed on many leukocyte subsets throughout the human immune system, and caution is therefore warranted when using antibody-therapy directed against this protein. The function of GPA33 still needs to be elucidated, but from

our data, we speculate that it may have a role in localization of undifferentiated T cells and/or in helping maintain their undifferentiated state.

Materials and methods

Antibodies

All antibodies used for CYTOF and flow cytometry are listed in Tables S1–S3. The FACS panels were designed in house for a different study (A. Kroeze, A. W. Turksma, N. Weterings, D. Stalder, C. Homburg, A. ten Brinke, C.E. van der Schoot, S.S. Zeerleder, C. Voermans, Cellular subsets in acute Graft-versus-Host disease, manuscript in preparation; and [16,17]) and slightly altered for the purpose of our experiments. Anti-GPA33 was obtained from the Olivia Newton-John Cancer Research Institute, Heidelberg, AU [36] and was labeled with Alexa Fluor® 647 Succinimidyl Ester (ThermoFisher Scientific). The commercially available GPA33 antibodies were validated with an isotype control (Rat IgG2A AF488 & Rat IgG2A PE, R&D systems) to identify the positive population, and binding to the target protein GPA33 was validated through transfection of HEK293T cells with a GPA33 construct (Figure S1). Anti-granzyme B was labeled with AF700 by Exbio (Prague, Czech Republic).

Sample preparation

Human material was obtained in accordance with the Declaration of Helsinki and Dutch regulation with respect to the use of human materials from volunteer donors. Buffy coats from healthy anonymized donors were obtained after their written informed consent, as approved by Sanquin's institutional ethical board. Peripheral blood mononuclear cells (PBMCs) were isolated using a Ficoll-Paque Plus (GE Healthcare) gradient. For long-term storage in liquid nitrogen, samples were frozen in 10% DMSO.

Flow cytometry

After careful thawing in 20% FCS/80% IMDM, cells were incubated with FcR Blocking Reagent (Miltenyi Biotec) for 10 min at room temperature. Surface staining of cells was done in PBS containing 0.5% FCS for 15 min at room temperature, except for CCR7, which was stained for 15 min at 37°C. To exclude dead cells from the analysis, Near IR (Life Technologies) was used as a Live/Dead marker. For intracellular staining of transcription factors, ki67 and Granzyme B, cells were fixed and permeabilized after surface staining with the Transcription factor buffer set (BD Pharmingen) following manufacturer's instructions. To measure cytokine production, cells were washed with culture medium

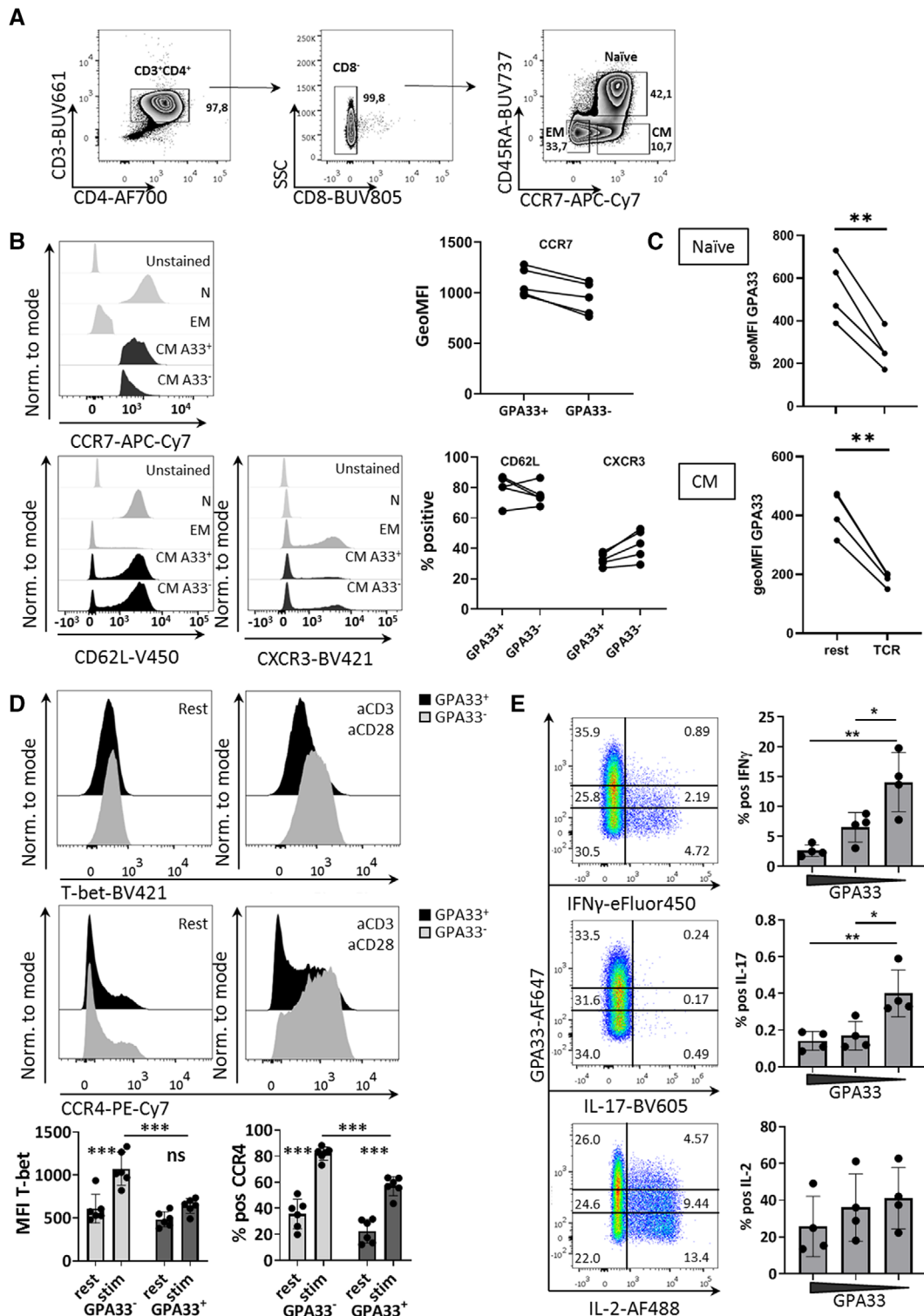


Figure 8. GPA33 identifies CD4⁺ Tcm cells lack effector capacity. (A) Gating strategy used to select naïve (N), effector memory (EM) and GPA33⁺ and GPA33⁻ central memory (CM) T cells from CD4⁺ MACSed cells. Selection of CD3⁺CD4⁺ T cells was done from the lymphocyte/single cell/live gate (not shown). Naïve, EM and GPA33⁺ and GPA33⁻ CM T cells were analysed for expression of CCR7, CD62L, and CXCR3 (B). All populations from a representative donor, including an unstained control, are shown at the top. The cumulative results from five donors, tested in two independent experiments are shown on the bottom. Expression of surface markers is either represented as GeoMFI of the total population (CCR7; bottom left) or as % positive (CD62L and CXCR3; bottom right). (C) Expression of GPA33 after overnight stimulation with 0,1 µg/ml aCD3 and 0,1 µg/ml aCD28 in 4 donors in one experiment. (D) Expression of T-bet and CCR4 on pre-sorted GPA33⁺ (black) and GPA33⁻ (grey) CM T cells are shown in histograms for a representative donor after being rested (left) or stimulated O/N with aCD3/aCD28 as in (C; right). Below the histograms, the cumulative results of all donors are shown. A total of 6 donors were tested in two independent experiments. Statistical comparisons were performed by one-way

and stimulated with 20 ng/ml Phorbol 12-myristate 13-acetate (PMA; Sigma) and 1 μ M Ionomycin (IM; Sigma) in the presence of Brefeldin A Solution (eBioscience) for 4h at 37°C. Anti-CD3 mAb (Pelicuster; 0.1 μ g/ml) and anti-CD28 mAb (eBioscience; 0.1 μ g/ml) were used to mimic antigen-specific T cell stimulation and co-stimulation, respectively. Cells were stimulated with these antibodies in IMDM overnight at 37°C. Data were acquired on an LSR Fortessa cytometer (BD Biosciences), and analyzed using the FlowJo software (version 10; Tree Star). Data were analyzed and reported according to chapter VII “Data handling, evaluation, storage & repositories” of the EJI Guidelines for the use of flow cytometry [37].

Cell sorting

CD4 microbeads (Miltenyi Biotec) were used for magnetic sorting according to the manufacturer’s instructions in order to extract CD4⁺ cells after isolation of PBMCs. Viable CD4⁺ T cell subsets were FACSorted on a FACS Aria III (BD Biosciences) after magnetic isolation of CD4⁺ cells, based on surface expression of a Live/Dead marker, CD25, CD127, CCR7, CD45RA, and/or GPA33.

CyTOF

PBMCs were thawed in 50% fetal calf serum and 50% IMDM. Thereafter, cells were spun for 7 min at 1500 RPM and recovered in IMDM with 10% human serum. The CyTOF antibody staining panel consisted of 39 surface markers including lineage, differentiation and activation markers (Table S3). Metal-conjugated antibodies were either purchased or conjugated. Per sample, 2×10^6 cells were stained for CyTOF acquisition as described previously [38]. Stained samples were stored pelleted in cell staining buffer for maximally 2 days before acquisition on the Helios. Live and single cells were distinguished using DNA stains and Gaussian discrimination parameters (residual and width) using the FlowJo software (version 10; Tree Star). Beads were excluded and cells were gated to be CD45⁺ for further analysis. Dimensionality reduction technique HSNE implemented in Cytosplore [39] was used for analysis of the dataset. Values were arcsine transformed before HSNE analysis based on 39 markers. Clusters were generated using the Gaussian-mean-shift method and further explored in-depth at different hierarchical levels in the HSNE analysis. HSNE maps and heatmaps were generated from the CD4⁺ and CD8⁺ T cell populations at level 3 and level 2 of the HSNE hierarchy, respectively.

Transfection of HEK293T cells

HEK293T cells were transfected with pMX-sv40-puro containing a GPA33 construct or an empty vector. Cells were maintained in DMEM+10% FCS and plated as 8×10^4 cells per well in a 24-wells plate in a total volume of 500 μ l for transfection. The next day, 103 μ l of 0.020 μ g/ μ l plasmid solution in OptiMEM was diluted 1:1 with 2.2 μ g of construct DNA per transfection. FuGENE (6.6 μ l) was added to each transfection. This mixture was incubated for 10 min at room temperature. Next, 25 μ l of the mixture was added per well. On day 4, all cells were trypsinated and analyzed by flow cytometry for expression of GPA33 using anti-GPA33 antibodies labeled with AF647, FITC, or PE and their respective isotype controls.

Acknowledgments: We would like to thank Mette Hazenberg and Vera van Hoven for their expert opinion on the ILC data, Martijn Nolte for advice, and Anja ten Brinke and Naomi Weterings for helping to set up and validate the FACS panels. This work was partly supported by grants from the Landsteiner Foundation for Blood Cell Research to DA (LSBR 1430, LSBR 1818). Furthermore, J.S. and B.R. are financed by the Dutch Diabetes Research Foundation and Foundation DON (Expert Center Grant, 2013.40.1693), T.N. and J.J.Z. are financed by the Dutch Arthritis Foundation (Research Center of Excellence program, LLP-16). A.K. was supported by Sanquin Research (PPOC13-027 grant). A Fellowship from the Landsteiner Foundation for Blood Transfusion Research to CV (grant no. #1101) also supported part of this work. A.M.S. is supported by an NHMRC Investigator Grant (No: 1177837). The graphical abstract was created with the BioRender software.

Conflict of interest: A patent application for the use of GPA33 to select Treg cells for clinical use has been filed by D.A. B.R. is the director of the Wanek Family Project for Type 1 Diabetes. All other authors have no commercial or financial conflict of interest.

Peer review: The peer review history for this article is available at <https://publons.com/publon/10.1002/eji.202048744>.

Data availability statement: The data that support the findings of this study are available from the corresponding author upon reasonable request.

ANOVA, followed by Sidak correction. *** $p < 0.001$. (E) Total CD4⁺ cells were stimulated with PMA+IO for 4 hours, followed by intracellular staining for IL-17, IFN γ and IL-2. Cytokines are plotted against GPA33 in the CM gate. Note that GPA33 expression does not change during this time frame. The graphs next to the flow cytometry plots depict the average production of each effector cytokine per GPA33 intensity (high to low, left to right on graphs) for four donors of one technical replicate from one experiment. Error bars represent mean \pm SD. Statistical comparisons were performed by one-way ANOVA, followed by Tukey’s HSD. * $p < 0.05$, ** $p < 0.01$. (for IL-17: GPA33^{hi} vs GPA33^{low} $p = 0.0078$; GPA33^{int} vs GPA33^{low} $p = 0.0152$; for IFN- γ : GPA33^{hi} vs GPA33^{low} $p = 0.0019$; GPA33^{int} vs GPA33^{low} $p = 0.0227$). All experiments were measured by flow cytometry.

References

- Xu, Z., Jin, B. A novel interface consisting of homologous immunoglobulin superfamily members with multiple functions. *Cell. Mol. Immunol.* 2010. 7: 11–19.
- Chrétien, I., Marcuz, A., Courtet, M., Katevuo, K., Vainio, O., Heath, J. K., White, S. J., et al. CTX, a *Xenopus* thymocyte receptor, defines a molecular family conserved throughout vertebrates. *Eur. J. Immunol.* 1998. 28: 4094–4104.
- Heath, J. K., White, S. J., Johnstone, C. N., Catimel, B., Simpson, R. J., Moritz, R. L., Tu, G. F., et al. The human A33 antigen is a transmembrane glycoprotein and a novel member of the immunoglobulin superfamily. *Proc. Natl. Acad. Sci. U. S. A.* 1997. 94: 469–474.
- Prasad, D. V. R., Nguyen, T., Li, Z., Yang, Y., Duong, J., Wang, Y., Dong, C., Murine B7-H3 Is a Negative Regulator of T Cells. *J. Immunol.* 2014. 173: 2500–2506.
- Vogt, L., Schmitz, N., Kurrer, M. O., Bauer, M., Hinton, H. I., Behnke, S., Gatto, D., et al. VSIG4, a B7 family-related protein, is a negative regulator of T cell activation. *J. Clin. Invest.* 2006. 116: 2817–2826.
- Lyons, P., Peters, J., Alberici, F., Liley, J., Coulson, R., Astle, W., Baldini, C., et al. Genetically distinct clinical subsets, and associations with asthma and eosinophil abundance, within Eosinophilic Granulomatosis with Polyangiitis. *bioRxiv.* 2018. 491837.
- Nguyen, C. Q., Cornelius, J. G., Cooper, L., Neff, J., Tao, J., Lee, B. H., Peck, A. B., et al. Identification of possible candidate genes regulating Sjögren's syndrome-associated autoimmunity: A potential role for TNFSF4 in autoimmune exocrinopathy. *Arthritis Res. Ther.* 2008. 10: R137.
- Williams, B. B., Tebbutt, N. C., Buchert, M., Putoczki, T. L., Doggett, K., Bao, S., Johnstone, C. N., et al. Glycoprotein A33 deficiency: a new mouse model of impaired intestinal epithelial barrier function and inflammatory disease. *Dis. Model. Mech.* 2015. 8: 805–815.
- Pereira-Fantini, P. M., Judd, L. M., Kalantzis, A., Peterson, A., Ernst, M., Heath, J. K., Giraud, A. S., et al. A33 antigen-deficient mice have defective colonic mucosal repair. *Inflamm. Bowel Dis.* 2010. 16: 604–612.
- Fan, G., Wang, Z., Hao, M., Li, J., et al. Bispecific antibodies and their applications. *J. Hematol. Oncol.* 2015. 8: 130.
- Moore, P. A., Shah, K., Yang, Y., Alderson, R., Roberts, P., Long, V., Liu, D., et al. Development of MGD007, a gpA33 x CD3-bispecific DART protein for T-cell immunotherapy of metastatic colorectal cancer. *Mol. Cancer Ther.* 2018. 17: 1761–1772.
- Wu, Z., Guo, H. F., Xu, H., Cheung, N. K., V. Development of a tetravalent anti-GPA33/anti-CD3 bispecific antibody for colorectal cancers. *Mol. Cancer Ther.* 2018. 17: 2164–2175.
- Masopust, D., Picker, L. J., et al. Hidden Memories: Frontline Memory T Cells and Early Pathogen Interception. *J. Immunol.* 2012. 188: 5811–5817.
- Agematsu, K., Nagumo, H., Yang, F. C., Nakazawa, T., Fukushima, K., Ito, S., Sugita, K., et al. B cell subpopulations separated by CD27 and crucial collaboration of CD27 + B cells and helper T cells in immunoglobulin production. *Eur. J. Immunol.* 1997. 27: 2073–2079.
- Marcenaro, E., Notarangelo, L. D., Orange, J. S., Vivier, E., et al. Editorial: NK cell subsets in health and disease: New developments. *Front. Immunol.* 2017. 8: 1363.
- Marius Munneke, J., Björklund, A. T., Mjösberg, J. M., Garming-Legert, K., Bernink, J. H., Blom, B., Huisman, C., et al. Activated innate lymphoid cells are associated with a reduced susceptibility to graft-versus-host disease. *Blood.* 2014. 124: 812–821.
- Hazenbergh, M. D., Spits, H., et al. Human innate lymphoid cells. *Blood.* 2014. 124: 700–709.
- Overgaard, N. H., Jung, J.-W., Steptoe, R. J., Wells, J. W., et al. CD4+/CD8+ double-positive T cells: more than just a developmental stage? *J. Leukoc. Biol.* 2015. 97: 31–38.
- Opstelten, R., de Kivit, S., Slot, M. C., van den Biggelaar, M., Iwaszkiewicz-Grześ, D., Gliwiński, M., Scott, A. M., et al. GPA33: A Marker to Identify Stable Human Regulatory T Cells. *J. Immunol.* 2020. 204: 3139–3148.
- Miyara, M., Yoshioka, Y., Kitoh, A., Shima, T., Wing, K., Niwa, A., Parizot, C., et al. Functional Delineation and Differentiation Dynamics of Human CD4+ T Cells Expressing the FoxP3 Transcription Factor. *Immunity.* 2009. 30: 899–911.
- Miles, B., Connick, E., et al. Control of the germinal center by follicular regulatory T cells during infection. *Front. Immunol.* 2018. 9: 2704.
- Chen, Y., Yu, M., Zheng, Y., Fu, G., Xin, G., Zhu, W., Luo, L., et al. CXCR5+PD-1+ follicular helper CD8 T cells control B cell tolerance. *Nat. Commun.* 2019. 10: 4415.
- Sojka, D. K., Bruniquel, D., Schwartz, R. H., Singh, N. J., et al. IL-2 Secretion by CD4+ T Cells In Vivo Is Rapid, Transient, and Influenced by TCR-Specific Competition. *J. Immunol.* 2004. 172: 6136–6143.
- Buchholz, V. R., Schumacher, T. N. M., Busch, D. H., et al. T Cell Fate at the Single-Cell Level. *Annu. Rev. Immunol.* 2016. 34: 65–92.
- Rivino, L., Messi, M., Jarrossay, D., Lanzavecchia, A., Sallusto, F., Geginat, J., et al. Chemokine receptor expression identifies pre-T helper (Th)1, pre-Th2, and nonpolarized cells among human CD4+ central memory T cells. *J. Exp. Med.* 2004. 200: 725–735.
- McLane, L. M., Banerjee, P. P., Cosma, G. L., Makedonas, G., Wherry, E. J., Orange, J. S., Betts, M. R., et al. Differential Localization of T-bet and Eomes in CD8 T Cell Memory Populations. *J. Immunol.* 2013. 190: 3207–3215.
- Lumsden, J. M., Schwenk, R. J., Rein, L. E., Moris, P., Janssens, M., Ofori-Anyinam, O., Cohen, J., et al. Protective immunity induced with the RTS,S/AS vaccine is associated with IL-2 and TNF- α producing effector and central memory CD4+ T cells. *PLoS One.* 2011. 6: e20775.
- Joly, E., Hudrisier, D., et al. What is trogocytosis and what is its purpose? *Nat. Immunol.* 2003. 4: 815.
- Mathieu, M., Martin-Jaular, L., Lavie, G., Théry, C., et al. Specificities of secretion and uptake of exosomes and other extracellular vesicles for cell-to-cell communication. *Nat. Cell Biol.* 2019. 21: 9–17.
- Sallusto, F., Geginat, J., Lanzavecchia, A., et al. Central Memory and Effector Memory T Cell Subsets: Function, Generation, and Maintenance. *Annu Rev Immunol.* 2004. 22: 745–763.
- Geginat, J., Paroni, M., Maglie, S., Alfen, J. S., Kastir, I., Gruarin, P., de Simone, M., et al. Plasticity of human CD4 T cell subsets. *Front. Immunol.* 2014. 5: 630.
- ElTanbouly, M. A., Zhao, Y., Nowak, E., Li, J., Schaafsma, E., Le Mercier, I., Ceeraz, S., et al. VISTA is a checkpoint regulator for naïve T cell quiescence and peripheral tolerance. *Science (80-).* 2020. 367: eaay0524.
- Sallusto, F., Lenig, D., Förster, R., Lipp, M., Lanzavecchia, A., et al. Two subsets of memory T lymphocytes with distinct homing potentials and effector functions. *Nature.* 1999. 401: 708–712.
- Smigiel, K. S., Richards, E., Srivastava, S., Thomas, K. R., Dudda, J. C., Klonowski, K. D., Campbell, D. J., et al. CCR7 provides localized access to IL-2 and defines homeostatically distinct regulatory T cell subsets. *J. Exp. Med.* 2014. 211: 121–136.
- Klinger, A., Gebert, A., Bieber, K., Kalies, K., Ager, A., Bel, E. B., Westermann, J., et al. Cyclical expression of L-selectin (CD62L) by recirculating T cells. *Int. Immunol.* 2009. 21: 443–455.
- Herbertson, R. A., Tebbutt, N. C., Lee, F.-T., Gill, S., Chappell, B., Cavicchiolo, T., Saunderson, T., et al. Targeted Chemoradiation in Metastatic Colorectal

Cancer: A Phase I Trial of 131I-huA33 with Concurrent Capecitabine. *J. Nucl. Med.* 2014. 55: 534–539.

- 37 Cossarizza, A., Chang, H. D., Radbruch, A., Acs, A., Adam, D., Adam-Klages, S., Agace, W. W., et al. Guidelines for the use of flow cytometry and cell sorting in immunological studies (second edition). *Eur. J. Immunol.* 2019. 49: 1457–1973.
- 38 van Unen, V., Li, N., Molendijk, I., Temurhan, M., Höllt, T., van der Meulen-de Jong, A. E., Verspaget, H. W., et al. Mass Cytometry of the Human Mucosal Immune System Identifies Tissue- and Disease-Associated Immune Subsets. *Immunity.* 2016. 44: 1227–1239.
- 39 Van Unen, V., Höllt, T., Pezzotti, N., Li, N., Reinders, M. J. T., Eisemann, E., Koning, F., et al. Visual analysis of mass cytometry data by hierarchical stochastic neighbour embedding reveals rare cell types. *Nat. Commun.* 2017. 8: 1740.

Abbreviations: **DC:** dendritic cell · **GPA33:** glycoprotein A33 · **HSNE:** Hierarchical Stochastic Neighbor Embedding · **ILC:** innate

lymphoid cell · **NK:** natural killer · **PBMC:** peripheral blood mononuclear cell · **PMA:** phorbol 12-myristate 13-acetate · **Tcm:** central memory T · **Tconv:** conventional T · **Tfh:** T follicular helper · **Tfr:** T follicular regulatory · **Treg:** regulatory T

Full correspondence: Derk Amsen, Amsterdam UMC, University of Amsterdam, location AMC, Department of Experimental Immunology, Amsterdam institute for Infection and Immunity, Meibergdreef 9, Amsterdam, The Netherlands. e-mail: d.amsen@amsterdamumc.nl; d.amsen@sanquin.nl

Received: 11/5/2020

Revised: 13/1/2021

Accepted: 10/3/2021

Accepted article online: 17/3/2021